DE-93-4-4

A NUMERICAL SIMULATION MODEL FOR STUDYING THE THERMAL PERFORMANCE OF WINDOWS

T.F. Smith, Ph.D.
Member ASHRAE

C. Beckermann, Ph.D.

C.C. Adams
Member ASHRAE

ABSTRACT

This paper presents a numerical simulation model that allows the impact of various design parameters on the thermal performance of windows to be evaluated. The model is for two-dimensional, combined conductive, convective, and radiative heat transfer and determines velocity profiles, temperatures, heat fluxes, and U-factors for the window. The window consists of two glass panes, a space between the glass panes containing a gas, and a sash. The effects of gas type, spacing between the glass panes, a low-emittance coating on one glass pane, sash designs, cladding strips, and between-glass-panes horizontal bar and vertical partition are reported. Comparisons are made to a one-dimensional model. Results from the model provide a more detailed picture of the thermal performance of a window and suggest design options that enhance the thermal performance of a window.

INTRODUCTION

The window is a building component that represents a desirable feature from the standpoint of natural daylighting, aesthetics, safety, and solar energy gain. If not properly designed and specified, the window could represent a significant percentage of heating energy lost during the winter and account for a significant amount of air-conditioning energy spent during the summer. Window technology has advanced during the past two decades with the development of double-pane windows, low-emittance coatings, between-glass-panes blinds and films, and gas-filled spaces. The effectiveness of further designs could be limited by the use of one-dimensional models for window heat transfer and the need for empirical testing, neither of which lends itself to generalized studies of window heat transfer processes. A second factor affecting window design is the development of a uniform system for rating window energy efficiency, resulting in a window labeling system. Antinori (1991) reports that as many as six labels are being considered, including the U-factor (ASHRAE 1989), and that a window testing procedure is being developed to determine the U-factor. Performing such tests, however, can be prohibitively expensive given the wide range of window designs and configurations. As a result of advances in technology and the impending window labeling system, comprehensive numerical simulation models are needed to provide (1) a more complete understanding of heat transfer processes in windows and (2) a method to reduce the number of tests.

Several currently available window heat-transfer simulation models may be classified as one-dimensional. Curcija et al. (1989) have reviewed their attributes. Such models are convenient for examining the effects on window heat transfer of glass emittance, films, number of glass panes, and types of gas filling enclosures between glass panes. Recent additions to the models include approximate methods for accounting for edge and frame effects. These models, however, do not account adequately for such factors as the interaction between the glass and the frame and for the convection that exists on the interior-facing surface. Edge effects and frame heat transfer become more important as the center-glass U-factors are reduced. Because the overall U-factor for a window is highly sensitive to these factors, more comprehensive simulation models are required. Current window designs that may include blinds, films, and decorative bars placed between glass panes and that consider window settings provide additional reasons to examine in greater detail the heat transfer processes common to windows.

Several multidimensional models with intended application to window heat-transfer processes have been reported. A comprehensive review of articles that discuss topics of interest to window heat-transfer applications is outside the scope of this paper. Where possible, this review concentrates on articles that have considered the simultaneous interaction of conductive, convective, and radiative heat transfer. Some articles may have been overlooked due to their inaccessibility. Wright and Sullivan (1989) have reviewed the literature concerned with natural convection in enclosures with particular attention paid to window heat transfer applications. Studies that considered two-dimensional natural convective flow in the enclosure formed by two glass panes are those of Ortega (1982, 1983), Korpela et al. (1982), and Lauriat and Desrayaud (1985), where isothermal vertical panes were assumed, and Behnia et al. (1985a, 1985b), where the inner pane was held isothermal and the outer pane had heat loss by convection and radiation. Marballi et al. (1984) examined heat transfer through a double-pane window including natural convective flow

Theodore F. Smith is a professor and **Christoph Beckermann** is an associate professor in the Department of Mechanical Engineering, University of Iowa, Iowa City. **Charles C. Adams** is an associate professor in the Engineering Department, Dordt College, Sioux Center, IA.

between the two glass panes and uniform convection coefficients on the exterior and interior surfaces. Yeoh et al. (1989) described a model for examining heat transfer through a double-pane window including natural convective flow between the two glass panes and a vertically varying convection coefficient on the inward-facing surface of the inner pane. Radiative heat transfer was neglected in the latter two studies. Results reported by Marballi et al. (1984) and Yeoh et al. (1989) are applicable for glass panes with an emittance of zero. Varapaev (1987) considered a double-pane window with radiant exchange between the two glass panes and fixed convection coefficients on the exterior and interior surfaces. Kangni et al. (1991) examined natural convection and conduction in rectangular enclosures containing multiple partitions. Zhang et al. (1991) reported heat-transfer results for enclosures containing a vertical, permeable screen. Carpenter and McGowan (1989) used a numerical simulation model based on conduction to obtain the heat transfer for window sashes. Elmahdy (1990) presented results of experimental and simulation studies for the overall U-factors for several window designs. Curcija (1992) developed a three-dimensional simulation model for window heat transfer with spatially varying heat transfer coefficients on the inner and outer panes and radiant exchange between the glass panes. Results were reported for two window designs. Although these studies do find applications, models of heat transfer in windows that examine a wide range of boundary conditions and designs are needed.

The overall purpose of this study is to develop a numerical simulation model for heat transfer processes common to window applications. The model reported in this paper accounts for two-dimensional heat transfer processes including natural convection, conduction, and radiation. The interaction of the various window components is included in the model. Results and findings of this study are restricted to those window designs considered.

The analysis, including a system description, a statement of the governing equations, and the boundary conditions, is given in the next section. The numerical solution procedure is then discussed. In the following section, values of the parameters appearing in the model for window designs considered in this study are specified, and numerical results for these window designs are presented and discussed.

ANALYSIS

System Description

A schematic diagram of the double-pane window considered in this study is shown in Figure 1. The window has a horizontal width, W, and a vertical height, H. Components of the window are exterior and interior glass panes, sashes, spacers, cladding strips, air cavities, and thermal breaks. The size of a component is described by its width and height in the x- and y-directions, respectively. Upper and lower spacers used to separate the glass panes could be separate or an integral part of the sash. Each lower and upper sash may have an exterior cladding strip that covers the exterior portion of the sash and an air cavity that is centered within the sash. Thermal breaks may appear in the sash. When there are no air cavities, the thermal break, if present, extends over the height of the sash. When an air cavity exists, thermal breaks are placed only within the solid, horizontal portions of the sash. Either a horizontal bar (for decorative purposes) or a vertical partition (representing a low-emittance plastic film or closed blinds) may be placed in the space between the glass panes. The exterior surfaces of the window have convective and radiative heat transfer with an exterior environment at a temperature of T_{ext}. The interior surfaces exchange heat by convection and radiation with an interior environment at T_{int}. The horizontal surfaces at the top and bottom of the window are considered adiabatic. Gravity acts in the negative y-direction. Gases occupying the space between the glass panes and the air cavities are radiatively nonparticipating. All surfaces exposed to radiatively nonparticipating gases, including the exterior- and interior-facing surfaces, are radiatively opaque, gray, and diffusely emitting and reflecting.

Governing Equations

A single-solution domain covering the entire window from $x = 0$ to W and $y = 0$ to H in Figure 1 is considered. The conservation equations describing two-dimensional fluid

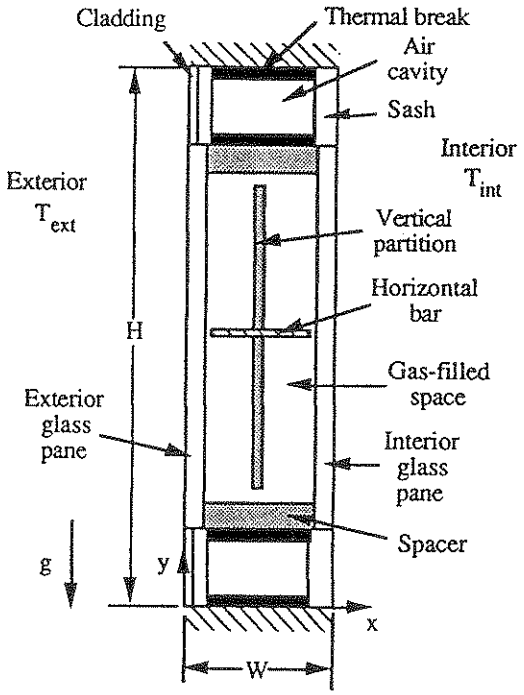

Figure 1 Schematic diagram of window.

flow and heat transfer for a rectangular solution domain for laminar flow, steady-state conditions, and no heat generation are

continuity:

$$\frac{\partial}{\partial x}(\rho u) + \frac{\partial}{\partial y}(\rho v) = 0 \tag{1}$$

x-momentum:

$$\rho u \frac{\partial u}{\partial x} + \rho v \frac{\partial u}{\partial y} = \frac{\partial}{\partial x}\left[\mu \frac{\partial u}{\partial x}\right] + \frac{\partial}{\partial y}\left[\mu \frac{\partial u}{\partial y}\right] - \frac{\partial P}{\partial x} \tag{2}$$

y-momentum:

$$\rho u \frac{\partial v}{\partial x} + \rho v \frac{\partial v}{\partial y} = \frac{\partial}{\partial x}\left[\mu \frac{\partial v}{\partial x}\right] + \frac{\partial}{\partial y}\left[\mu \frac{\partial v}{\partial y}\right] - \frac{\partial P}{\partial y} + \rho g \beta (T - T_{ref}) \tag{3}$$

energy:

$$\rho u c_P \frac{\partial T}{\partial x} + \rho v c_P \frac{\partial T}{\partial y} = \frac{\partial}{\partial x}\left[k \frac{\partial T}{\partial x}\right] + \frac{\partial}{\partial y}\left[k \frac{\partial T}{\partial y}\right] - \nabla \cdot \vec{q}_r \tag{4}$$

where the Boussinesq approximation is applied. The thermophysical properties of density ρ, specific heat c_P, dynamic viscosity μ, coefficient of volumetric expansion β, and thermal conductivity k depend on the material present at a particular x,y location. Gas properties are evaluated at the mean of the exterior and interior ambient temperatures. For the density, the gases are assumed to obey the ideal gas equation of state. The remaining gas properties are taken from Incropera and DeWitt (1990) for air and Touloukian et al. (1970a, 1970b) and Touloukian and Makita (1970) for argon. Temperature-independent properties are assumed for all solid materials. In solid materials, the viscosity is set to a very large value to force the velocities to vanish. The velocity components in the x- and y-directions are u and v, respectively. This procedure for handling conjugate heat-transfer problems is discussed in more detail in Patankar (1980). The value of the reference temperature T_{ref} does not affect the solutions. The last term in Equation 4 is the divergence of the radiative flux. Because the gas is assumed to be radiatively transparent and the solid materials to be opaque, the radiative flux is nonzero only at gas/solid interfaces.

Boundary Conditions

The boundary conditions for the velocities are

$$u, v = 0 \tag{5}$$

at all solid boundaries. The general boundary condition for the energy equation at the boundary of the solution domain is

$$-k \frac{\partial T}{\partial n} = h_c (T - T_\infty) - \varepsilon_s \sigma (T^4 - T_\infty^4) \tag{6}$$

where n is the coordinate normal to the boundary, h_c is the convection coefficient, T is the temperature of the boundary, T_∞ is the surrounding temperature (T_{ext} or T_{int}), ε_s is the emittance at the boundary, and σ is the Stefan-Boltzmann constant.

At the adiabatic boundary along the bottom and top sashes, Equation 6 applies, but $h_c = 0$ and $\varepsilon_s = 0$. For some cases, the sashes in Figure 1 are removed and the adiabatic boundary is applied directly to the ends of the glass panes and the space between the glass panes. For this situation, the temperature distribution along the adiabatic surface is determined from an energy balance that considers conduction with the adjacent gas or glass elements and radiant exchange (only when an adjacent element is a gas) with the other surfaces forming the enclosure. The portion of the adiabatic surface exposed to the gas is taken to be impervious and black.

Along the exterior-facing surface, the convection coefficient in Equation 6 is taken as a constant to simulate a forced-convection situation. For the interior-facing surface, the convective coefficient may be assigned a constant value or may be allowed to vary in the y-direction. The expression for the vertically varying convection coefficient for the interior surface is taken from Yeoh et. al. (1989) and is written as

$$h_c = k C \left[\frac{g \beta}{\nu \alpha}\right]^{1/4} [T(z) - T_{int}]^{2/3} \div \left\{\int_0^z [T(z') - T_{int}]^{5/3} dz'\right\}^{1/4} \tag{7}$$

where k, β, ν ($= \mu/\rho$), and α ($= k/\rho/c_P$) are properties of the interior gas taken as air at atmospheric pressure and $T(z)$ is the temperature distribution along the surface with z measured from the start of the boundary layer. The temperature for evaluating the air properties is the mean of $T(z)$ and T_{int}. The Prandtl number function, C, is given by

$$C = 0.563/[1 + (0.437/\mathrm{Pr})^{9/16}]^{4/9} \tag{8}$$

where Pr ($= c_P \mu/k$) is the Prandtl number. For the parameters (discussed later) addressed in this paper, the boundary layer starts at $y = H$.

Radiation Fluxes

The two-dimensional radiative transport equation for the intensity for an absorbing and emitting medium within the solution domain is

$$\mu \frac{\partial I}{\partial x} + \eta \frac{\partial I}{\partial y} = -\kappa I + \kappa I_b \tag{9}$$

where $I = I(x,y;\ \mu,\eta)$, μ and η are direction cosines, κ is the absorption coefficient of the medium, and I_b is the blackbody intensity. Opaque and transparent media are represented by large and small values of the absorption coefficient, respectively. For a large value of the absorption coefficient, the intensity equals the blackbody intensity, and for an absorption coefficient of zero, the intensity remains unchanged. At an opaque surface, the intensity leaving is composed of the emitted intensity and the reflected irradiation and is written as

$$I(x_a,y_a;\mu,\eta) = \varepsilon I_b(x_a,y_a) + \frac{\rho}{\pi}\int_{2\pi} I'(x_a,y_a;\mu',\eta')\cos\phi'\,d\omega' \quad (10)$$

where subscript a denotes a surface, ε is the surface emittance, and ρ is the surface reflectance ($= 1 - \varepsilon$). The prime denotes an incoming quantity, ϕ is the polar angle between the surface normal and the intensity, and ω is the solid angle. The integration in Equation 10 is performed over the hemisphere above the surface.

The net radiant energy leaving an opaque surface is

$$q_r(x_a,y_a) = \int_{2\pi} I(x_a,y_a;\mu,\eta)\cos\phi\,d\omega - \int_{2\pi} I'(x_a,y_a;\mu',\eta')\cos\phi'\,d\omega', \quad (11)$$

which represents the difference between the leaving and arriving radiant energy.

Overall Heat Transfer Coefficient

The overall heat transfer coefficient for the window, commonly referred to as the U-factor, is defined by

$$U = q_t/[H(T_{ext} - T_{int}] \quad (12)$$

where q_t is the heat transfer through the window. The heat transfer through the window is based on the sum of the convective and radiative heat flows from the boundary of the domain and is expressed by

$$q_t = \int_0^H \left\{h_c[T(y) - T_\infty] + \varepsilon\sigma[T^4(y) - T_\infty^4]\right\}dy, \quad (13)$$

which applies to either of the domain boundaries, $x = 0$ or $x = W$. From the problem statement, the exterior and interior heat transfer rates are identical.

NUMERICAL PROCEDURE

The finite-volume method of Patankar (1980) is used to solve the governing equations for the fluid flow and for conductive and convective heat transfer. Special procedures are required to incorporate the surface radiative heat fluxes into the method (Beckermann and Smith 1992). A radiative heat transfer model based on the discrete-ordinates method developed for application to radiant exchange between surfaces separated by a transparent medium (Sánchez and Smith 1992) is incorporated in the flow and heat transfer model. The numerical model has been exercised for a variety of geometries and boundary conditions. The accuracy of the portion of the model for flow and heat transfer by conduction and convection has been verified by House et al. (1990). The accuracy of the radiation model has been discussed by Sánchez and Smith (1992). Results for the combined models are in good agreement with exact, analytical, and other numerical solutions for natural convection and radiation in a square cavity and for natural convection and radiation in enclosures and vertical channels. As an example, consider natural convection in a square enclosure with the vertical walls maintained at uniform, but different, temperatures and the horizontal walls adiabatic. For combined natural convection and surface radiant exchange in the enclosure with a Rayleigh number of 0.7×10^5 and with black walls, Fusegi and Farouk (1987) cite an overall Nusselt number of 27.6, whereas the present code gives 26.71. For a second example, consider an open, vertical channel with walls maintained at uniform, but different, temperatures. For black walls, a Grashof number of 100 based on the aspect ratio, a Prandtl number of 0.7, an aspect ratio of 1000, a temperature ratio of 1.1, and a radiation-to-conduction ratio of 1.5 (see Sparrow et al. [1980] for definitions of the five dimensionless parameters), Sparrow et al. cite a dimensionless convective heat transfer of 4.0×10^{-2} and the present model gives 3.74×10^{-2}.

The numerical grid for the window heat-transfer simulation is selected to ensure accurate results without excessive computational times. Within the vertical gas space, a nonuniform grid spacing in the x-direction with a finer grid near solid surfaces is chosen to increase the accuracy of the numerical results. The nonuniform grid was generated using a power law with an exponent of 1.5. For most results, 20 control volumes are assigned to the horizontal direction for the space and three to a glass pane. For the vertical direction, 60 control volumes are assigned to the space. The number of control volumes for the sash depends on the thermal conductivity and the presence of an air cavity. For example, the grid spacing for the horizontal and vertical directions is 5 mm (0.20 in.) for a solid wood sash and 1 mm (0.04 in.) for an aluminum sash of 1 mm (0.04 in.) thickness. The number of discrete directions per octant for the radiation model is 10. Doubling the number of control volumes and discrete directions produced U-factors that differ by less than 0.2%. Computational time for the central processor unit is typically 1,500 seconds on a computer system with four 7.5-megaflop processors and 64-Mb RAM. The window heat-transfer code consists of three programs. A preprocessing program allows for convenient changing of the window design and aids in entering the window configuration into the flow and heat

transfer program. The flow and heat transfer program computes and outputs the velocity and temperature fields. A post-processing program operates on the outputs of the flow and heat transfer program to compute heat fluxes and U-factors.

PARAMETERS

A window has a wide range of designs and is exposed to a wide range of environmental conditions. To aid in comparing the thermal performance of windows, a set of standard conditions has been defined (ASHRAE 1989). The standard conditions for a wintertime environment are $T_{ext} = -17.8°C$ (0°F) and $T_{int} = 21.1°C$ (70°F) with a 6.67-m/s (15-mph) wind on the exterior surface. This wind creates an exterior convective coefficient of 29.0 W/m^2·K (4.2 Btu/h·ft^2·°F) (ASHRAE 1989). Practical ranges for overall window heights and spacings are 0.3 to 1.2 m (1 to 4 ft) and 3 to 25 mm (0.125 to 1 in.), respectively. Unless otherwise noted, the gas in the space is air at atmospheric conditions. Results for windows with argon filling the space are also presented. The air cavities in Figure 1 contain air at atmospheric pressure. Gas properties are evaluated at the mean temperature of T_{ext} and T_{int}. Values of thermal conductivities and emittances for materials found in window construction and used in this study, unless otherwise noted, are cited in Table 1. For glass, emittances are specified for standard glass and for a glass surface with a low-emittance coating. Phenolic material is used as a thermal break. Coated aluminum is used for the cladding strips.

TABLE 1
Material Description and Property Values†

Material	Property	SI		EE
Glass	Thermal conductivity*	0.90		0.52
	Emittance		0.84	
	Emittance (low-e)		0.1	
Wood	Thermal conductivity	0.14		0.081
	Emittance		0.9	
Phenolic resin	Thermal conductivity	0.22		0.13
	Emittance		0.9	
Polystyrene	Thermal conductivity	0.16		0.091
	Emittance		0.9	
Aluminum	Thermal conductivity	170		98
	Emittance		0.1	
Aluminum with coating	Thermal conductivity	170		98
	Emittance		0.1	

† Values for the properties were obtained by consulting ASHRAE (1989), Incropera and DeWitt (1990), and other sources. Properties found in the literature for these materials do vary and representative values are used.

* Thermal conductivity has units of W/m·K for International System of Units (SI) and Btu/h·ft·°F for English Engineering Units (EE)

RESULTS AND DISCUSSION

To demonstrate the model's validity and capabilities, several design variations of the window depicted in Figure 1 are examined. Effects of coatings on the glass pane, the type of gas within the space, the material properties used to construct the cladding strips and sash, and the size, placement, and thermophysical properties of the horizontal bar and vertical partition are of interest. Though the number of possible designs is large, only a limited number of cases are presented to illustrate the influence of some of the more important design factors. Results of interest include the U-factors, the heat fluxes for the exterior and interior surfaces, and the velocity and temperature distributions. For comparison with previously reported findings, results for a double-glass-pane window without a sash are reported first. Cases that examine various sash constructions are then presented, followed by results for windows that include a horizontal bar or a vertical partition.

Double-Glass Panes

A double-glass-pane window (DGP) consists of only two glass panes each with a width of 3 mm (0.118 in.) and separated by a distance of 15 mm (0.59 in.). The height of the window is 300 mm (11.8 in.). For reference, the glass pane surfaces are numbered 1 to 4, where 1 refers to the exterior facing surface of the exterior pane. The window heat-transfer model gives a U-factor of 2.960 W/m^2·K (0.521 Btu/h·ft^2·R). This U-factor agrees favorably with that cited for the center glass U-factor (2.90 W/m^2·K [0.51 Btu/h·ft^2·°F]) for identical conditions (Johnson 1992) and, as shown in Table 2, the U-factor from a one-dimensional model (LBL 1988).

Replacing the air in the space with argon at atmospheric pressure produces a U-factor of 2.761 W/m^2·K (0.486 Btu/h·ft^2·°F), or a 7% reduction when compared to the U-factor with air in the space. For a coating on surface 3 with an emittance of 0.1, the U-factor is 2.039 W/m^2·K (0.359 Btu/h·ft^2·°F), indicating a reduction of about 31% in the U-factor due to the low-emittance coating. As shown in Table 2, for argon in one case and a low-emittance coating in another, the U-factors obtained from the one-dimensional model (LBL 1988) and the current model are in good agreement. This agreement, however, is highly dependent on selecting the proper correlations for the convective coefficients in the one-dimensional model. The remaining results are for standard glass panes with air occupying the space.

A capability of the current model is a vertically varying convection coefficient for surface 4. For the double-glass-pane configuration with a vertically varying convective coefficient, the temperature of surface 4 varies from 275.2 to 285.2 K (495 to 513 R) at $y = 2.5$ to 297.5 mm (0.098 in. to 11.8 in.). Assuming a linear variation of the surface temperature between the temperatures cited for $y = 0$ and

TABLE 2
Comparison of U-Factors for No Sashes

Window design	U	
	W/m²·K	Btu/h·ft²·°F
Double glass panes (air)		
Window 3.1 (1988)	2.785	0.490
Current model	2.960	0.521
Double glass panes (argon)		
Window 3.1 (1988)	2.610	0.460
Current model	2.761	0.486
Double glass panes (air, low-e: 0.1)		
Window 3.1 (1988)	1.820	0.321
Current model	2.039	0.359

300 mm, the local convection coefficient calculated from Equation 7 ranges from h_c = 3.60 to 7.27 W/m²·K (0.63 to 1.28 Btu/h·ft²·°F) at y = 2.50 and 297.5 mm (0.098 and 11.7 in.), respectively, and the average convection coefficient is 4.02 W/m²·K (0.71 Btu/h·ft²·°F). For a constant convection coefficient on surface 4 equal to 4.02 W/m²·K (0.71 Btu/h·ft²·°F), the simulations for the DGP window give U = 2.971 W/m²·K (0.523 Btu/h·ft²·°F) and the temperatures for surface 4 vary from 275.7 to 284.0 K (496 R to 511 R) at y = 2.50 and 297.5 mm (0.098 and 11.7 in.), respectively. This finding indicates that the U-factor for a constant convection coefficient on surface 4 is similar to that for a vertically varying convection coefficient (2.960 W/m²·K (0.521 Btu/h·ft²·R). This finding does not necessarily imply that a constant convection coefficient could be used because obtaining an accurate average value, even if a Nusselt number correlation is used, may not be easy. For an isothermal surface at 280 K (504 R), the range of the average convection coefficients obtained from the Nusselt number correlations for natural convection from a vertical isothermal surface (Incropera and DeWitt 1990) is 3.51 to 3.97 W/m²·K (0.62 to 0.70 Btu/h·ft²·°F). The average convection coefficient from the vertically varying correlation in Equation 7 lies just outside the upper limit of this range. Unless otherwise noted, succeeding results assume a vertically varying convection coefficient on surface 4.

Results that demonstrate the effect of the width of the gas-filled space on the U-factor are reported in Figure 2. The results labeled "constant h" are for a convection coefficient on surface 4 equal to a constant value of 4.02 W/m²·K (0.71 Btu/h·ft²·°F). This value is based on the previously mentioned average value for the vertically varying coefficient. Results for the vertically varying and constant convection coefficients display the expected behavior with spacing, namely: as the spacing increases, the U-factor diminishes from the conduction region near a space width of 5 mm (0.19 in.) to a minimum at about 14 mm (0.59 in.), increases as convection becomes important, and then decreases at larger spacings. For comparison, the U-factors at a spacing of 25 mm (0.98 in.) from the current model and the one-dimensional model are 2.99 and 2.84 W/m²·K (0.53 and 0.50 Btu/h·ft²·°F). The minimum U-factors for the variable and constant convection coefficient cases occur near a spacing of 14 mm (0.59 in.). The Rayleigh number (Incropera and DeWitt 1990), based on the space width and the difference between the averages of the temperatures for surfaces 2 and 3, is near 320 at 5 mm (0.19 in.), 10,000 at 15 mm, and 48,000 at 25 mm (0.98 in.), implying laminar flow within the space.

Sash Effects

The effect of a sash is examined by adding sashes of 21 mm (0.83 in.) width and 30 mm (1.18 in.) height to the bottom and top of the double-glass pane. All other conditions are the same. The horizontal adiabatic boundary conditions are now applied along the outside horizontal surfaces of the sashes. For a wooden sash, the simulations yield a U-factor of 2.999 W/m²·K (0.528 Btu/h·ft²·°F), which is about the same as that for the double-glass pane. The similarity between the U-factors of the double-glass-pane window with and without sashes is due to the larger surface areas for the glass than for the sashes. Although the wooden sash does not significantly alter the U-factor for the window, the effect of the sash on the fluxes along surfaces 1 and 4 is of interest. Heat fluxes for the exterior and interior surfaces (1 and 4) of the lower and upper sash and glass are shown in Table 3 (part a). The sums of the products of the heat flux and corresponding area for the exterior and interior surfaces are equal. The exterior and interior glass heat fluxes are nearly identical. The heat fluxes for the sashes are greater than those for the glass except for surface 1 of the lower sash. Because of this, even though the sash has a smaller area, the sash may be an important

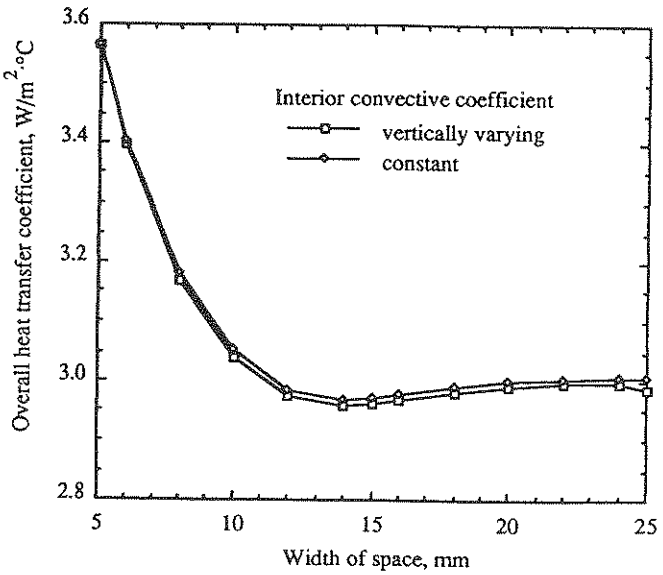

Figure 2 Effect of width of gas-filled space.

TABLE 3
Heat Fluxes and U-Factors for Various Sash Options for Air-Filled Spaces

Surface	Heat transfer, Exterior	W/m² Interior	U, W/m² · K (Btu/h · ft² · °F)
(a) Sash (wood)			
Upper sash	156.48	133.49	2.999
Glass	113.41	113.68	(0.528)
Lower sash	112.04	133.23	
(a.1) Sash (h_c = 4.02 W/m² · K)			
Upper sash	148.06	121.46	3.034
Glass	115.46	115.94	(0.534)
Lower sash	117.3	139.27	
(b) Sash (wood) and spacers			
Upper sash	148.15	140.46	3.036
Glass	115.58	115.19	(0.0534)
Lower sash	118.66	130.44	
(c) Sash (wood), spacers, and cladding strips			
Upper sash	159.34	143.18	3.049
Glass	114.74	115.34	(0.537)
Lower sash	122.99	132.79	
(d) Sash (wood), spacers, and cladding strips, air cavity (15 × 24 mm)			
Upper sash	147.09	123.91	2.987
Glass	114.59	115.31	(0.526)
Lower sash	106.41	121.85	
(e) Sash (aluminum), spacers, cladding strips, air cavity (19 × 28 mm)			
Upper sash	313.02	245.60	3.498
Glass	112.93	124.31	(0.616)
Lower sash	210.13	156.16	
(f) Sash (aluminum), spacers, cladding strips, air cavity (19 × 28 mm)			
Upper sash	134.03	99.26	2.859
Glass	111.81	115.72	(0.503)
Lower sash	85.62	78.69	
(g) Sash (aluminum), spacers, cladding strips, polystyrene cavity (19 × 28 mm), thermal break (15 × 1 mm)			
Upper sash	163.21	125.56	2.977
Glass	112.03	117.28	(0.524)
Lower sash	112.37	94.00	

factor in the overall heat transfer through the window. For the lower sash, the heat flux at the interior surface is higher than that at the exterior surface. The reverse is found for the upper sash. Also, the heat flux from surface 1 of the upper sash is higher than that for the lower sash. The behavior of the heat fluxes along surface 4 is attributed to the vertically varying convection coefficient on surface 4, which, because of the boundary layer effect, is higher for the upper sash than for the lower sash. Because the glass heat fluxes are nearly identical, a portion of the heat transferred to surface 4 of the lower sash is conducted to surface 1 on the lower sash and the remainder is convected and radiated to the upper sash where it then contributes to the heat flux for surface 1 of the upper sash. This finding suggests that it may be beneficial to have separate designs for the lower and upper sashes, with the upper sash being a better insulator.

To account for sash effects, the calculation of the U-factor for the entire window using a one-dimensional model is based on the sum-of-area-weighted-U-factor method (ASHRAE 1989) using the center-glass, edge, and sash U-factors. To examine the applicability of this method to the current results, the overall U-factor for the window is approximated by

$$U_T = (A_g U_g + A_s U_s)/(A_g + A_s) \qquad (14)$$

where A_g and A_s are the glass and sash areas and U_g and U_s are the U-factors for the glass and sash regions. Edge effects are assumed to be accounted for by U_g. The U-factors for the sash and glass are calculated separately and, therefore, the simultaneous interaction between the sash, glass panes, and gas in the space is not taken into account in Equation 14. For one-dimensional conduction within the wood sash, the same interior and exterior conditions as cited, and an interior convective coefficient of 4.02 W/m²·K (0.71 Btu/h·ft²·°F), the U-factor for the sash is 3.400 W/m²·K (0.599 Btu/h·ft²·°F). For the glass, the U-factor is taken from that computed for the double-glass pane, that is, U_g = 2.960 W/m²·K (0.521 Btu/h·ft²·°F). For the sash and glass areas (A_s = 60 mm = 2.36 in. and A_g = 300 mm = 11.8 in.) used for the results in Table 3 (part a), the U-factor from Equation 14 is 3.033 W/m²·K (0.534 Btu/h·ft²·°F). Note that this U-factor is nearly identical to that cited in Table 3 using the two-dimensional model. This finding does not necessarily imply that Equation 14 is always valid. The applicability of Equation 14 rests on the equality of the center-glass heat fluxes in Table 3 (part a) and the compensating effect of the heat fluxes for the upper and lower sashes.

The effect of changing the convection coefficient for surface 4 from one that varies vertically to a constant (4.02 W/m²·K [0.71 Btu/h·ft²·°F]) is shown in Table 3 (part a1). For a constant convection coefficient, the U-factor increases slightly from that in Table 3 and the glass heat fluxes increase by about 2%. The lower (upper) sash heat fluxes for surface 4 increase (decrease) by about 5% (9%). In agreement with the results in Table 3 (part a), the heat flux for surface 1 of the upper sash is the highest of all of the sash heat fluxes. This finding is attributed to the natural convection within the space, where the air within the space that is heated as it flows upward along the interior pane transfers a part of its thermal energy to the upper sash as it flows in the negative x-direction past the upper sash.

In Table 3 (part b), spacers between the glass panes are added at the top and bottom of the space for the window in Table 3 (part a). Each spacer is 15 mm (0.59 in.) wide and 10 mm (0.39 in.) high and is assigned the thermal properties of wood. The air space height is maintained at 300 mm

(11.8 in.), and the glass panes are each extended to a height of 320 mm (12.6 in.). The full height of the window is 380 mm (15.0 in.). The U-factor for the double-glass panes with the sash and spacers is 3.036 W/m^2·K (0.534 Btu/h·ft^2·°F) and the heat fluxes are given in Table 3 (part b). The glass heat fluxes are for a glass height of 320 mm (12.6 in.). The spacers result in higher glass heat fluxes, and the sum of the lower and upper sash heat-transfer rates increases only slightly when compared to those in Table 3 (part a). Succeeding cases include the spacers as described above.

In some windows, cladding strips are added to the exterior surfaces of a sash to reduce the maintenance associated with the wood sash. Results in Table 3 (part c) are for cladding strips, each 1 mm (0.04 in.) wide and constructed of coated aluminum (see Table 1). The U-factor for this window is 3.035 W/m^2·K (0.534 Btu/h·ft^2·°F), which is about 0.4% higher than that for a sash without a cladding strip (Table 3, part b). Because of the small contact area with the cladding strips, the glass heat fluxes (Table 3, part c) are not affected by them. The sash heat fluxes all experience an increase when compared to those in Table 3 (part b). It is noteworthy that the heat flux for surface 1 of the upper sash has increased by about 8% when compared to that in Table 3 (part b).

In an attempt to reduce the heat transfer associated with the sash, an air cavity 15 mm (0.59 in.) wide and 24 mm (0.94 in.) high is centered in the wood sash. For this cavity size, the sash surrounding the cavity has a thickness of 3 mm (0.12 in.). Natural convective and radiative exchange occurs within the cavity. From Table 3 (part d), the U-factor for this window is 2.987 W/m^2·K (0.523 Btu/h·ft^2·°F), which is only slightly lower than that when the cavity is not considered (Table 3, part c). Examination of the heat fluxes in Table 3 (part d) reveals that the fluxes for the sash decrease considerably. Because the sash area is relatively small when compared to the glass area, the overall U-factor experiences only a slight decrease when the air cavity is added. Further reduction in the sash heat fluxes may be possible by painting the surfaces surrounding the cavity with a low-emittance paint to reduce radiation effects and by filling the cavity with a low-thermal-conductivity material to reduce natural convection effects.

The influence of the sash material is shown in Table 3 (part e) for an aluminum sash 1 mm (0.04 in.) thick surrounding an air cavity 19 mm (0.74 in.) wide and 28 mm (1.10 in.) high. Because of its high thermal conductivity, it would be impractical to use a solid aluminum sash. Cladding strips of coated aluminum 1 mm (0.04 in.) wide are used for the exterior surface. The backside of a cladding strip is exposed to the air cavity and is assigned an emittance of 0.9. The other three aluminum surfaces surrounding the cavity have an emittance of 0.1. Because of the high thermal conductivity of aluminum, the overall U-factor is 3.498 W/m^2·K (0.616 Btu/h·ft^2·°F) and the heat fluxes for the sash surfaces increase significantly as shown in Table 3 (part e). The heat flux for surface 1 of the upper sash is the highest at 313.02 W/m^2 (99 Btu/h·ft^2). These findings illustrate the interrelationship between the thermal characteristics of the glass panes and the sash.

In an attempt to reduce the U-factor for the aluminum sash listed in Table 3 (part e), thermal breaks constructed of phenolic resin (Table 1) are centered in the horizontal portions of the sash. A thermal break is 15 mm (0.59 in.) wide and 1 mm (0.04 in.) high. The thermal break reduces the U-factor to 2.859 W/m^2·K (0.503 Btu/h·ft^2·°F) with a significant reduction in the sash heat fluxes (see Table 3, part f). The glass heat flux for surface 4 is now similar to that for a wood sash (Table 3, part b). When compared to results in Table 3 (part e), the addition of the thermal breaks reduces the heat flux for surface 4 of the upper sash by more than 50%. To reduce natural convection and radiant exchange in the air cavity, thereby possibly producing a smaller U-factor, the cavity is filled with an opaque material with properties similar to those of polystyrene (Table 1). As shown in Table 3 (part g), the U-factor for this window construction is higher by about 4% than that for the air cavity (Table 3, part f). An air-filled insulation material that has a lower thermal conductivity and is radiatively opaque could be tried in the air cavity as a means to reduce the U-factor. From these results, the low-emittance surfaces of the aluminum sash in conjunction with the air cavity and thermal break yields the lowest U-factor for windows with an aluminum sash. It may be possible to lower the U-factor further by removing the high-emittance coating on the backside of the cladding strip and filling the cavity with an opaque material of low thermal conductivity.

To illustrate other model results, plots of streamlines and isotherms for the window with a wood sash containing an air cavity (Table 3, part d) are illustrated in Figure 3a for the entire solution domain. To aid in interpreting the plots, the window configuration (the left-most diagram) has been provided. Because of plotting and reproduction limitations, there is not a perfect match between the sizes of the three diagrams. The streamlines indicate that there are three cells, one for each air cavity and one for the space. The maximum value of the stream function of the cell in the space is 0.556 kg/m·s (0.37 lb$_m$/ft·s) found near the center of the space; that in the lower air cavity is near 0.19 kg/m·s (0.13 lb$_m$/ft·s); and that in the upper air cavity is about 0.20 kg/m·s (0.13 lb$_m$/ft·s). The airflow in the cells is counterclockwise. The isotherms in Figure 3a range from 257 K (3°F) near the exterior surface to 284 K (51°F) near the interior surface. The lower areas of the interior glass pane have temperatures near 276 K (37°F), which favor formation of condensation. The isotherms in the air cavities and space display similar characteristics as those for natural convection in a vertical enclosure. The isotherms are more numerous in regions of larger temperature gradients found in the lower right and upper left corners of a cell. The nearly vertical isotherms in the spacers and adjacent sash indicate that conduction is nearly one-dimensional in the x-direction for these areas.

Horizontal Bar

Results for a horizontal bar centered horizontally and vertically in a double-glass-pane window with a solid wood sash (21 by 30 mm [0.83 by 1.18 in.]) and spacer (15 by 10 mm [0.59 by 0.39 in.]) are reported in Table 4. Results in Table 4 (part a) are for a square bar with 8 mm (0.31 in.) sides and material properties of polystyrene. There are 3.5-mm (0.14-in.) gaps between the glass panes and the bar. Air flows in these gaps if conditions are favorable. In comparison with the results in Table 3 (part b), the addition of the bar increases the U-factor by about 1%. The glass heat fluxes experience an increase as a result of the bar.

Streamlines and isotherms for the window in Table 4 (part a) are displayed in Figure 3b. Because of the horizontal bar, lower and upper cells are formed; the addition of more streamlines (not shown here) indicates that there is a large cell, but of smaller intensity, flowing around the

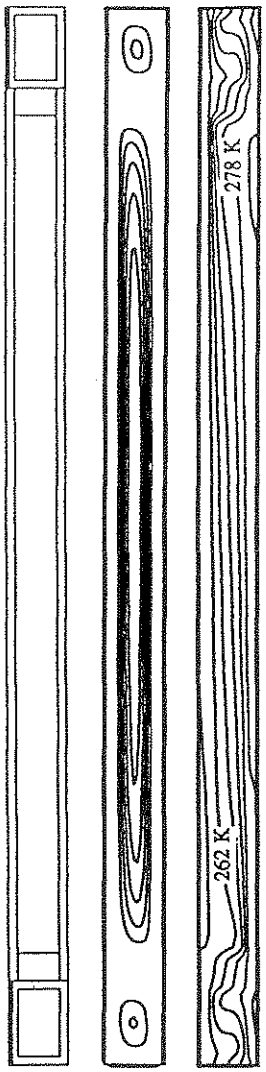

(a) Window with double-glass panes, spacers, sashes, air cavities, and cladding strips. Streamlines (min: 0.0 kg/m·s; max: 0.556 kg/m·s; 6 equal increments). Isotherms (equal increments of 4°C).

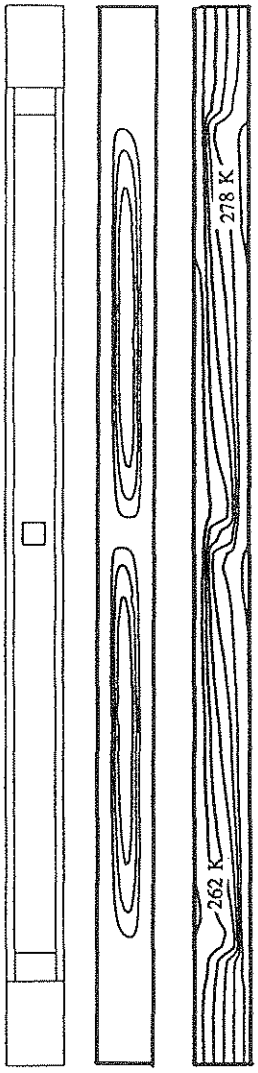

(b) Window with double-glass panes, spacers, sashes, air cavities, and a horizontal bar. Streamlines (min: 0.0 kg/m·s; max: 0.475 kg/m·s; 4 equal increments). Isotherms (equal increments of 4°C).

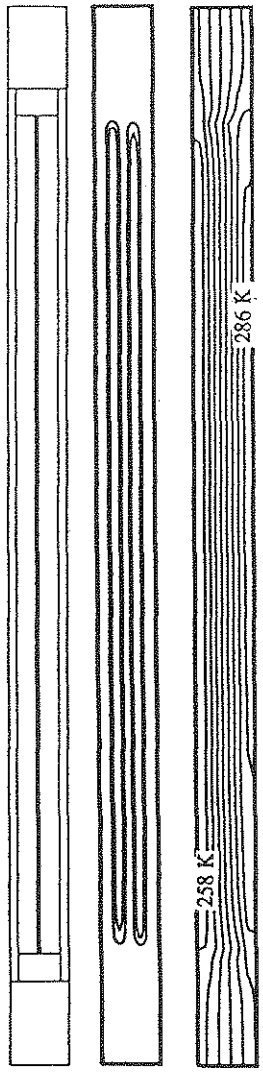

(c) Window with double-glass panes, spacers, sashes, air cavities, and a vertical partition. Streamlines (min: 0.0 kg/m·s; max: 0.058 kg/m·s; 3 equal increments). Isotherms (equal increments of 4°C).

Figure 3 *Window configuration (left), streamlines (center), and isotherms (right).*

TABLE 4
Heat Fluxes and U-Factors for Horizontal Bar

Surface	Heat transfer, Exterior	W/m^2 Interior	U, W/m2 · K (Btu/h · ft² · °F)
(a) Partial bar (8 × 8 mm)			
Upper sash	146.64	139.72	3.070
Glass	117.27	116.88	(0.541)
Lower sash	118.96	129.98	
(b) Full bar (15 ×1 mm)			
Upper sash	146.54	139.79	3.110
Glass	119.14	118.74	(0.548)
Lower sash	118.92	129.84	
(c) Full bar (15 × 1 mm): coated aluminum			
Upper sash	146.44	139.87	3.233
Glass	124.87	124.47	(0.569)
Lower sash	118.61	129.54	
(d) Partial bar (13 × 1 mm): coated aluminum			
Upper sash	146.60	139.88	3.102
Glass	118.76	118.37	(0.546)
Lower sash	118.91	129.88	

entire space. The distortion of the isotherms near the center of the window indicates the location of the bar and indicates some conduction in the vertical direction through the bar. The temperatures range from 258 K (4°F) near the lower left corner to 281 K (46°F) near the interior glass pane.

To possibly suppress the natural convection in the space between the glass panes for the window design in Table 3 (part b), the bar could be extended across the space. In Table 4 (part b), a bar of polystyrene extends across the space and has a height of 1 mm (0.04 in.). Because the bar touches the glass panes, the U-factor and glass heat fluxes increase from those in Table 3 (part b). In Table 4 (part c), a coated aluminum bar of the same dimensions replaces the polystyrene bar in Table 4 (part b). The U-factor and heat fluxes for the glass surfaces are higher than those for the polystyrene bar. By placing 1-mm (0.04-in.) gaps on either side of the bar, whose width is then 13 mm (0.51 in.), a slight decrease in the U-factor is observed and the glass heat fluxes are reduced by about 5%, as shown in Table 4 (part d). For the window designs in Table 4, the bar is not effective in reducing the heat transfer across the window when compared to the results in Table 3 (part b).

Vertical Partition

The next window design considers the installation of a vertical partition in the space (e.g., a low-e film). The partition is 0.06 mm (0.002 in.) wide and 300 mm (11.8 in.) high and is constructed of a material having a thermal conductivity similar to that of polystyrene with an emittance of 0.1. The partition is placed midway between the glass panes for the window in Table 3 (part b) (with a wood sash and spacers) and extends from the bottom to the top of the space. Because of the low-emittance partition, results shown in Table 5 for the glass heat fluxes are near 63 W/m^2, a decrease of more than 40% from the partitionless results, and the U-factor for the window is 1.916 $W/m^2 \cdot K$ (0.337 $Btu/h \cdot ft^2 \cdot °F$).

Streamlines and isotherms for this window are presented in Figure 3c. A cell is found in each space on the left and right sides of the partition, and the maximum value of the stream function is reduced to 0.058 kg/m·s (0.039 $lb_m/ft \cdot s$), which is about an order of magnitude lower than that in Figure 3a. The isotherms are nearly parallel in the vertical direction, indicating that the heat transfer in the air is mostly by conduction. The temperatures range from near 257 K (3°F) on the exterior glass pane to 287 K (57°F) on the interior glass pane.

TABLE 5
Heat Fluxes and U-Factors for Vertical Partition

Surface	Heat transfer, W/m^2 Exterior	Interior	U, $W/m^2 \cdot K$ ($Btu/h \cdot ft^2 \cdot °F$)
Upper sash	144.06	139.96	1.916
Glass	63.26	63.82	(0.337)
Lower sash	127.92	126.96	

CONCLUSIONS

A numerical simulation model to study the thermal performance of windows has been presented. The model considers two-dimensional heat transfer by conduction, convection, and radiation and computes the local temperatures, gas velocities, and heat fluxes. Capabilities of the model include variable glass pane widths, heights, and spacings; various sash designs and materials; thermal breaks; vertically varying convective coefficients at the inner and outer surfaces; multiple gases; bars and partitions between the glass panes; and arbitrary thermophysical properties of all components. The effects of some of these design parameters on the window thermal performance have been investigated in detail. For certain limiting cases, the model agrees well with results obtained from one-dimensional calculations and U-factors reported in the literature; however, the agreement depends highly on the choice of the average convection coefficient in the one-dimensional model and may be fortuitous in the presence of a sash. The present model provides insight into the local heat-transfer phenomena and the relative importance of the various heat-transfer modes and paths. The interrelations between and sensitivity to various design changes are easily examined. The model is expected to be a valuable tool in rating the thermal performance of windows, without the need for extensive tests. Future extensions of the model could include solar radiation, additional sash and frame designs, three-dimensional heat transfer, transient effects, and additional methods to

describe the interaction of the window with the environments.

REFERENCES

Antinori, C. 1991. Window labeling on the horizon. *Home Energy* 8(5): 11-12.

ASHRAE. 1989. *1989 ASHRAE handbook—Fundamentals*. Atlanta: American Society of Heating, Refrigerating and Air-Conditioning Engineers, Inc.

Beckermann, C., and T.F. Smith. 1993. Incorporation of internal surface radiant exchange in the finite volume method. *Numerical Heat Transfer* 23(B): 127-133.

Behnia, M., J.A. Reizes, and G. de Vahl Davis. 1985a. Natural convection in a cavity with a window. AIAA Paper No. 85-1073.

Behnia, M., J.A. Reizes, and G. de Vahl Davis. 1985b. Natural convection in a rectangular slot with convective-radiative boundaries. ASME Paper No. 85-HT-35.

Carpenter, S.C., and A.G. McGowan. 1989. Frame and spacer effects on window U-value. *ASHRAE Transactions* 95(1): 604-608.

Curcija, D. 1992. Three-dimensional finite element model of overall, night time heat transfer through fenestration systems. Ph.D. thesis, University of Massachusetts, Amherst.

Curcija, D., L.L. Ambs, and W.P. Goss. 1989. A comparison of European and North American window U-value calculation procedures. *ASHRAE Transactions* 95(1): 575-591.

Elmahdy, A.H. 1990. Joint Canadian/U.S. research project on window performance: Project outline and preliminary results. *ASHRAE Transactions* 96(1): 896-900.

Fusegi, T., and B. Farouk. 1987. Radiation-convection interactions of a non-gray gas in a square enclosure. *Heat and Mass Transfer in Fire*, ASME HTD-Vol. 73, pp. 63-68.

House, J.M., C. Beckermann, and T.F. Smith. 1990. Effect of a centered conducting body on natural convection heat transfer in an enclosure. *Numerical Heat Transfer*, Part A, Vol. 18, pp. 213-225.

Incropera, F.P., and D.P. DeWitt. 1990. *Fundamentals of heat and mass transfer*, 3d ed. New York: John Wiley & Sons.

Johnson, T.E. 1992. *Low-e glazing design guide*. Butterworth-Heinemann, Maine.

Kangni, A., R. Ben Yedder, and E. Bilgen. 1991. Natural convection and conduction in enclosures with multiple vertical partitions. *International Journal of Heat and Mass Transfer* 34(11): 2819-2825.

Korpela, S.A., Y. Lee, and J.E. Drummond. 1982. Heat transfer through a double pane window. *Journal of Heat Transfer* 104(3): 539-544.

Lauriat, G., and G. Desrayaud. 1985. Natural convection in air-filled cavities of high aspect ratios: Discrepancies between experimental and theoretical results. ASME paper No. 85-HT-37.

LBL. 1988. *Window 3.1, A PC program for analyzing window thermal performance*. Berkeley, CA: Windows and Daylighting Group, Applied Science Division, Lawrence Berkeley Laboratory, University of California.

Marballi, V.M., S.A. Korpela, Y. Lee, and S. Nakamura. 1984. Heat transfer through a vertical enclosure with convective boundary conditions. *International Journal of Heat and Mass Transfer* 27(12): 2431-2434.

Ortega, J.K.E. 1982. Thermal impedance of multi-pane windows. *Passive Solar Journal* 1(2): 121-127.

Ortega, J.K.E. 1983. Optimum spacing between low-emissive window panes. *Natural Convection in Enclosures—1983*, ASME HTD-Vol. 26, pp. 83-86.

Patankar, S.V. 1980. *Numerical heat transfer and fluid flow*. New York: McGraw-Hill Book Co.

Sánchez, A., and T.F. Smith. 1992. Surface radiation exchange for two-dimensional rectangular enclosures using the discrete-ordinates method. *Journal of Heat Transfer* 114: 465-472.

Sparrow, E.M., S. Shah, and C. Prakash. 1980. Natural convection in a vertical channel: 1. Interacting convection and radiation; 2. The vertical plate with and without shrouding. *Numerical Heat Transfer* 3: 297-314.

Touloukian, Y.S., and T. Makita. 1970. *Thermophysical properties of matter: Specific heat*, vol. 6. New York: Plenum.

Touloukian, Y.S., P.E. Liley, and S.C. Saxena. 1970a. *Thermophysical properties of matter: Thermal conductivity*, vol. 3. New York: Plenum.

Touloukian, Y.S., S.C. Saxena, and P. Hestermans. 1970b. *Thermophysical properties of matter: Viscosity*, vol. 11. New York: Plenum.

Varapaev, V.N. 1987. Convection and heat transfer in a vertical layer with allowance for radiation from non-isothermal walls. *Fluid Dynamics* 22(1): 19-24.

Wright, J.L., and H.F. Sullivan. 1989. Natural convection in sealed glazing units: A review. *ASHRAE Transactions* 95(1): 592-603.

Yeoh, G.H., G. de Vahl Davis, and E. Leonardi. 1989. Heat transfer across a double-glazed window with convective boundary conditions. *Numerical Methods in Thermal Problems* VI(1): 355-365.

Zhang, Z., A. Bejan, and J.L. Lage. 1991. Natural convection in a vertical enclosure with internal permeable screen. *Journal of Heat Transfer* 113(2): 377-383.

DISCUSSION

Leon Glicksman, Professor, Massachusetts Institute of Technology, Cambridge: Compare your solution to simple models, establish simple approximations, and establish areas where two-dimensional effects, etc., are more important.

T.F. Smith: During the development of the numerical model, we compared our results to those of one-dimensional models to validate the numerical model (some comparisons are cited in the paper). The plots of the streamlines and isotherms indicate that two-dimensional effects are important in regions separating the air space and the sash, in the air cavities of the sashes, and in the vertical bar.

Joseph Klems, Staff Scientist, Lawrence Berkeley Laboratory, Berkeley, CA: I found this a very interesting paper. What are the computer requirements of your code?

Smith: Computational time for the central processor unit is typically 1,500 seconds on a computer system with a 7.5-megaflop processor and 64 Mb RAM. The computer resources required to perform the calculations depend strongly on the number of control volumes.

Peter L. van der Mersch, Manager, Mechanical Engineering, University of Colorado, Boulder: How would you take into account the use of tinted glass, due to its heat-absorbing characteristics?

Smith: For tinted glass, the only properties needed for the model are the thermal conductivity and the emittances of both surfaces.

Hakim Elmahdy, Senior Research Officer, National Research Council of Canada, Ottawa, ON: How much time is needed to enter data for simple and complicated sash profiles? What are the limitations of this model? Large size (real windows) may result in multiple cells in the cavity. Will you investigate that in the future?

Smith: The numerical model is composed of three modules: (1) preprocessing, (2) processing, and (3) postprocessing. The processing module is restricted to two-dimensional rectangular geometries but allows for arbitrary properties of each control volume. Problem-specific attributes are entered in the preprocessing module. A single preprocessing module is used for the cases reported in the paper. If only minor changes from these cases are required, then the time to enter the new design is minimal. If a major redesign is required, it might take about one to two hours of my time to develop a new preprocessor module. We have examined the occurrence of multiple cells in tall windows but, for the paper, have not reported results for tall windows because of the extensive number of control volumes and resultant computer resources required. We plan to generalize the model to more complicated geometries and also report on the effects of multiple cells in the near future.